Journal of Materials Chemistry B

ROYAL SOCIETY OF CHEMISTRY

COMMUNICATION

View Article Online
View Journal | View Issue

Cite this: *J. Mater. Chem. B*, 2024, **12**, 6570

Received 22nd April 2024,
Accepted 15th June 2024

DOI: 10.1039/d4tb00872c

rsc.li/materials-b

Sensing cholesterol-induced rigidity in model membranes with time-resolved fluorescence spectroscopy and microscopy†

Bidisha Biswas,‡ Dhari Shah,‡ Sarah J. Cox-Vázquez and Ricardo Javier Vázquez *

Here, we report the characterization of cholesterol levels on membrane fluidity with a twisted intramolecular charge transfer (TICT) membrane dye, namely DI-8-ANEPPS, using fluorescence lifetime techniques such as time-correlated single photon counting (TCSPC) and fluorescence lifetime imaging microscopy (FLIM). The characterized liposomes comprised a 3 : 1 ratio of POPC and POPG, respectively, 1% DI-8-ANEPPS, and increasing cholesterol levels from 0% to 50%. Fluorescence lifetime characterization revealed that increasing the cholesterol levels from 0% to 50% increases the fluorescence lifetime of DI-8-ANEPPS from 2.36 ns to 3.65 ns, a 55% increment. Such lengthening in the fluorescence lifetime is concomitant with reduced Stokes shifts and higher quantum yield, revealing that localized excitation (LE) dominates over TICT states with increased cholesterol levels. Fluorescence anisotropy measurements revealed a less isotropic environment in the membrane upon increasing cholesterol levels, suggesting a shift from liquid-disorder (Lα) to liquid-order (LO) upon adding cholesterol. Local electrostatic and dipole characterization experiments revealed that changes in the zeta-potential (ζ-potential) and transmembrane dipole potential (Ψ_d) induced by changes in cholesterol levels or the POPC : POPG ratio play a minimal role in the fluorescence lifetime outcome of DI-8-ANEPPS. Instead, these results indicate that the cholesterol's effect in restricting the degree of movement of DI-8-ANEPPS dominates its photophysics over the cholesterol effect on the local dipole strength. We envision that time-resolved spectroscopy and microscopy, coupled with TICT dyes, could be a convenient tool in exploring the complex interplay between membrane lipids, sterols, and proteins and provide novel insights into membrane fluidity, organization, and function.

Introduction

Cholesterol plays a key role in modulating the fluidity and dipole potential in mammalian cell membranes,[1–4] which are fundamental physico-electrochemical properties associated with cellular communication, signaling, dysfunction, and trafficking.[5–11] Therefore, developing appropriate analytical methods and tools for characterizing cholesterol levels and its homeostasis is important. Traditional optical methods for sensing cholesterol include steady-state fluorescence spectroscopy coupled with membrane-intercalating molecular probes sensitive to such physico-electrochemical properties.[1,7,12] Of relevance is the visualization of voltage transients in membranes upon external stimuli, possible by a fluorescence ratiometric method.[3,13–15] This approach correlates the dye's fluorescence intensity ratio, R, with transmembrane dipole potential (Ψ_d).[1,16] Using this approach, it is recommended that the

Ricardo Javier Vázquez

Ricardo Javier Vázquez, an emerging scientist from Puerto Rico, pursued his doctoral studies at the University of Michigan, Ann Arbor, under Professor Theodore Goodson III's guidance. His research utilized time-resolved spectroscopy and non-linear optics to explore important properties in organic optoelectronic materials. Post-PhD, Ricardo undertook postdoctoral studies with Professor Guillermo C. Bazan at the National University of Singapore, focusing on water-soluble organic optoelectronic materials for bioimaging and energy applications. Now, at the Chemistry Department at Indiana University Bloomington, Ricardo's independent career bridges organic materials and measurement science to address problems regarding precision in life science, energy transduction, and bioelectronics.

Department of Chemistry, Indiana University, Bloomington, Indiana 47405, USA. E-mail: ricvazqu@iu.edu

† Electronic supplementary information (ESI) available. See DOI: https://doi.org/10.1039/d4tb00872c

‡ These authors contributed equally to this work.

overall excited state of the dye possess a mono-exponential decay with a lifetime <2 ns to minimize anisotropic contributions of the membrane and obtain a correct R estimation.[17]

An alternative method to study the fluorescence of a molecular probe is by characterizing the probes' lifetime using bulk time-resolved spectroscopic and microscopic techniques.[18–23] Note that the fluorescence lifetime is a concentration-independent property that could also be sensitive to changes in biological microenvironments.[24,25] The fluorescence lifetime imaging microscopy (FLIM) technique, which produces an image based on the differences in the fluorescence lifetime of a dye, has been used for characterizing cholesterol biophysics.[26–29] For example, subtle changes in the fluorescence lifetime of a molecular probe were associated with a steady increase in membrane fluidity observed in cancer cells during treatment.[30] Also, FLIM resolved subtle fluorescence lifetime variations from molecular probes accompanied by membrane lipid modification upon treatment.[31] These examples serve as seminal findings and accentuate the potential for using time-resolved techniques to extract information about the impact of cholesterol levels on the physico-electrochemical properties of biological membranes.[32] However, benchmark studies using time-resolved techniques to understand such properties are needed. To this end, we used DI-8-ANEPPS (Fig. 1A), which resides in parallel orientation with the lipids (Fig. 1B), as the molecular probe to systematically study how changing cholesterol levels influence the fluidity and transmembrane potential of biological membranes. Liposomes (100 nm) and giant multilamellar vesicles (GMLVs) composed of a 3 : 1 ratio of POPC : POPG, which are in fluid phase at room temperature, with cholesterol levels from 0% to 50%, were used for bulk time-resolved fluorescence spectroscopy and FLIM characterization, respectively. Complementary steady-state fluorescence techniques were also used for contextualization and further analysis. The technical details for liposome formulation and fluorescence characterization can be found in the ESI.†

Results revealed that increasing the cholesterol level within the lipid bilayer of the liposomes increases the fluorescence lifetimes of DI-8-ANEPPS, see Fig. 1C. The fluorescence lifetime as a function of cholesterol levels fits a Boltzmann sigmoidal distribution; see Fig. 1D and Fig. S1 (ESI†). Interestingly, a bi-exponential decay characteristic of chromophores with twisted intramolecular charge transfer (TICT) character better represented the fluorescence lifetime of DI-8-ANEPPS, see ESI.†[17,32–34] Note that the first decay component is short and close to the instrument response function (IRF), so the analysis was based on the second decay component. For context, the fluorescence lifetime of DI-8-ANEPPS systematically increased from 2.36 ns to 3.65 ns, a 55% fluorescence lifetime increment, when the cholesterol levels were systematically increased from 0% to 50%, respectively, see Table S1 (ESI†). Of relevance is evaluating the changes in the fluorescence lifetime of DI-8-ANEPPS in biologically relevant cholesterol levels (24% and 40%).[9,35] Note that when the cholesterol levels in the lipid bilayer were gradually increased from 24% to 40%, the fluorescence lifetime of DI-8-ANEPPS-intercalated liposomes gradually increased from 2.70 ns to 3.52 ns, see Fig. S2 (ESI†). These results were further corroborated with GMLVs using FLIM, see Fig. 2. Note that the fluorescence lifetimes captured by FLIM followed a similar trend to those obtained by bulk time-resolved spectroscopy, see Fig. S3 (ESI†), suggesting that the local microenvironment of DI-8-ANEPPS is similar at different membrane sizes. These results are important, as subtle

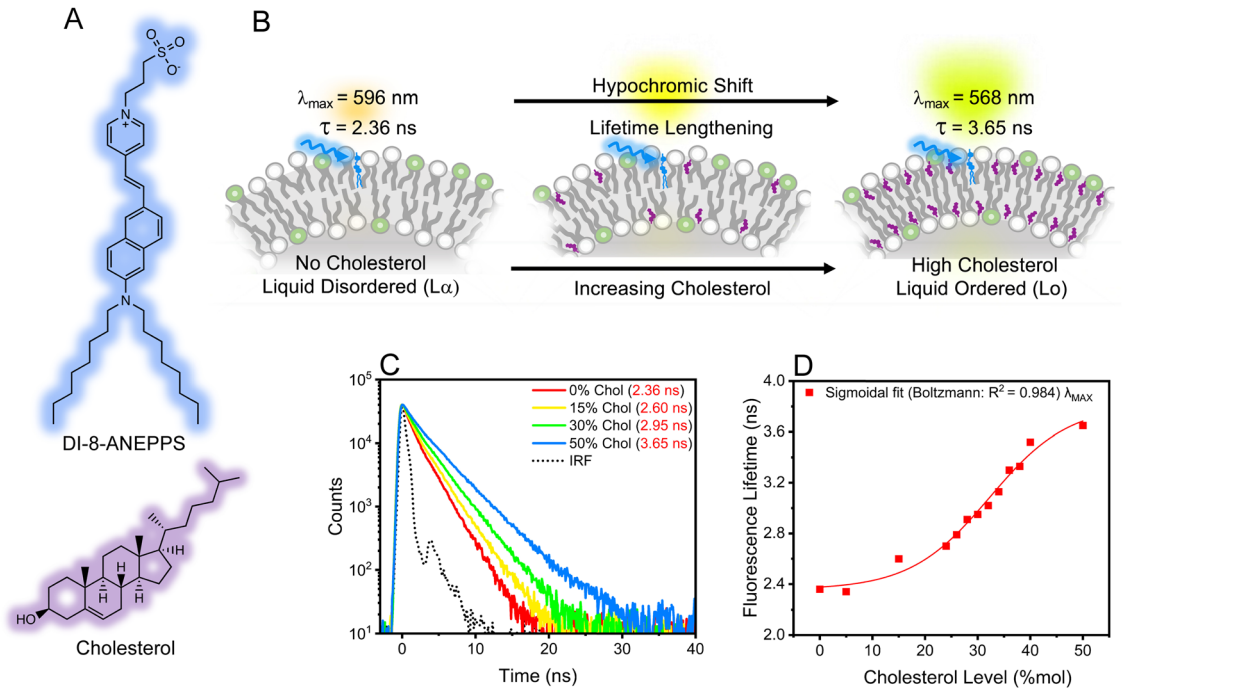

Fig. 1 (A) Molecular structures of DI-8-ANEPPS and cholesterol. (B) Both of these compounds reside perpendicular to the membrane surface. (C) Fluorescence lifetime profiles of the DI-8-ANEPPS-intercalated 100 nm extruded liposomes composed of a 3 : 1 ratio of POPC : POPG with cholesterol levels from 0% to 50%. (D) Boltzmann sigmoidal fit curve of the fluorescence lifetime in function of cholesterol levels.

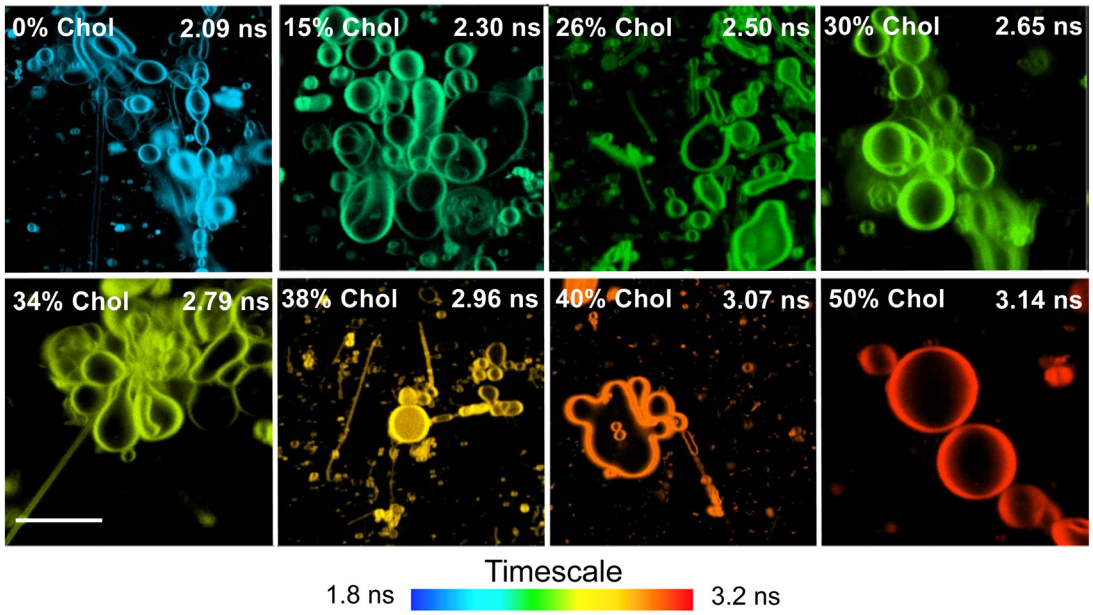

Fig. 2 Representative FLIM images for DI-8-ANEPPS-intercalated POPC:POPG GMLVs with different cholesterol levels. The scale bar is 10 μm.

changes in cholesterol levels at physiological conditions can be detected, resolved, and analyzed using time-resolved spectroscopy and microscopy techniques.

The TICT nature of DI-8-ANEPPS makes it an excellent candidate for evaluating anisotropic mediums, which means that the restrictions imposed by the microenvironment (membrane's fluidity) on the dynamic properties of the molecule could be characterized with fluorescence methods.[36] In the context of these experiments, an increment in fluorescence anisotropy ($F_{anisotropy}$) can represent a higher degree of structural order or low membrane fluidity.[37] The excitation wavelength for the analysis was the same used for the fluorescence lifetime characterization (456 nm), and the collection wavelength was the fluorescence λ_{MAX} of each sample (see ESI† for more information). Fig. S4 (ESI†) shows a positive correlation between cholesterol levels and $F_{anisotropy}$, which could explain the fluorescence lifetime trends, revealing that increasing cholesterol levels reduce the membrane's fluidity. Notably, the transition temperature for POPC (−2 °C) and POPG (−2 °C), the lipids used for creating the liposomes, is contextualized.[38] Liposomes composed of such lipids are in the fluid phase at room temperature (liquid-disordered phase – Lα), and increasing the cholesterol levels within their lipid bilayer could increase the membrane's rigidity (liquid-ordered phase – LO).[5,39] This becomes more apparent when complementary fluorescence features of DI-8-ANEPPS are considered. Note that this lengthening in the fluorescence lifetime of DI-8-ANEPPS upon increasing the cholesterol levels is concomitant with an increase in its fluorescence intensity (quantum yield), see Fig. S5 (ESI†). In addition, increasing cholesterol levels induced a hypsochromic shift with reduced full width at half maxima (FWHM) in the fluorescence spectrum of DI-8-ANPPES. Hypsochromic shifts in TICT are often associated with loss in the rotational freedom of the TICT state.[20] More importantly, a reduction in Stokes shifts was obtained upon increasing the cholesterol levels within the membrane, accentuating that localized excitation (LE) becomes dominant over TICT states. These fluorescence spectral features indicate that DI-8-ANEPPS is motion-restricted due to confinement within lipid domains, namely POPC and POPG, upon increasing cholesterol levels.[40–42] Such photophysical features indicate that increasing the cholesterol levels in liposomes composed of POPC:POPG results in membranes with more LO phase character than Lα character.

Increasing the cholesterol levels in the membrane may affect its dipole potential, influencing the membrane microenvironments where DI-8-ANEPPS resides and possibly convoluting the contributions from rigidity and dipole-induced fluorescence lifetimes.[2,13,14,17] Therefore, we investigated how cholesterol-induced changes in electrostatic interactions within the membrane may affect the fluorescence lifetime lengthening of DI-8-ANEPPS. The first parameter considered was the Zeta-potential (ζ-potential) of the investigated liposomes. Lipids are polyelectrolytes in a suspension that attract different ions to their surface, potentially changing the membrane dipole microenvironment upon excitation.[43–45] It is important to note that DI-8-ANEPPS is expected to reside in parallel with the lipids, the sulfonated group near the membrane-solution interface, while the non-polar hydrocarbon tails are localized within the hydrophobic core of the bilayer (Fig. 1B).[14] As shown in Fig. 3A, increasing the cholesterol levels in the investigated membranes minimally impacts their ζ-potentials. For example, the ζ-potential for the investigated liposomes with 0%, 15%, 30%, and 50% cholesterol levels are −59.4 mV, −52.9 mV, −59.4 mV, and −62.6 mV. No correlation between the ζ-potentials and any cholesterol-dependent photophysics was found.

Next, we designed liposomes with sizable differences in ζ-potential s. POPC has a zwitterionic lipid head group, while PG has a negatively charged lipid head group (Scheme S1, ESI†).

Therefore, it is possible to modify the ζ-potentials of the liposomes by altering the equimolar concentration between such lipids relative to that of the original liposomes (POPC : POPG – 3 : 1). To that end, liposomes with fixed cholesterol levels (15%) but with different lipids ratios (7 : 1, 3 : 1, 1 : 1, and 1 : 7) were generated. As expected, increasing the POPG ratio content in the liposomes relative to POPC resulted in liposomes with a more negative ζ-potential, see Fig. 3B. Changing the POPC : POPG ratios from 1 : 7 to 7 : 1 decreased the ζ-potential from −72.4 mV to −43.0 mV. This decrease in ζ-potential was concomitant to an increase in the fluorescence lifetime of DI-8-ANEPPS (from 2.52 ns to 2.60 ns), see Fig. 3C, highlighting the importance of electrostatic charges on the photophysics of DI-8-ANEPPS. However, the ζ-potential of the liposomes has minimal impact on the fluorescence lifetime of DI-8-ANEPPS compared to the influence that cholesterol-induced rigidity has on the lipid bilayer.

Cholesterol levels can impact Ψ_d of the liposomes, affecting the photophysics of DI-8-ANEPPS. While directly measuring Ψ_d is difficult, it can be estimated by its linear relationship with the fluorescence intensity ratio (R) of DI-8-ANEPPS when detected at the edge of its fluorescence spectra ($\lambda_{670\,nm}$) after excitation at the blue edge ($\lambda_{420\,nm}$) and red edge ($\lambda_{510\,nm}$) of its absorption spectrum, see eqn (1).[15]

$$\Psi_d = \frac{(R + 0.3)}{4.3 \times 10^{-3}} \quad (1)$$

It is believed that selecting these wavelengths minimizes membrane fluidity effects on R, which is further described in the ESI.† [1] As shown in Fig. 4A and Fig. S6 (ESI†), increasing the cholesterol levels in the membrane proportionally increases Ψ_d. For example, Ψ_d increases from 405 mV to 663 mV when cholesterol was increased from 0% to 50%, a 64% increment, suggesting that Ψ_d might contribute significantly to lengthening the fluorescence lifetime of DI-8-ANEPPS.

To address this proposition, we evaluated the influence of the POPC : POPG ratios on Ψ_d, see Fig. 4B and Fig. S7 (ESI†). Interestingly, liposomes with lower POPG content possess a higher Ψ_d. For example, systematically changing the POPC : POPG ratios from 1 : 7 to 7 : 1 increases Ψ_d from 432 mV to 495 mV. This Ψ_d increment is 15%, like that for those liposomes when cholesterol levels are increased from 0% to 15%, see Table S1 (ESI†). However, the fluorescence lifetime increments by modulating the POPC : POPG ratios are minimal compared to the impact of increasing cholesterol levels, see Fig. 1A and 3C. For example, there is a 0.08 ns increment in the fluorescence lifetime when the ratio of POPC : POPG is changed from 1 : 7 to 7 : 1, while the fluorescence lifetime increment when the cholesterol levels are increased from 0% to 15% is three times larger at 0.24 ns. These results suggest that a cholesterol-induced reduction in membrane fluidity might

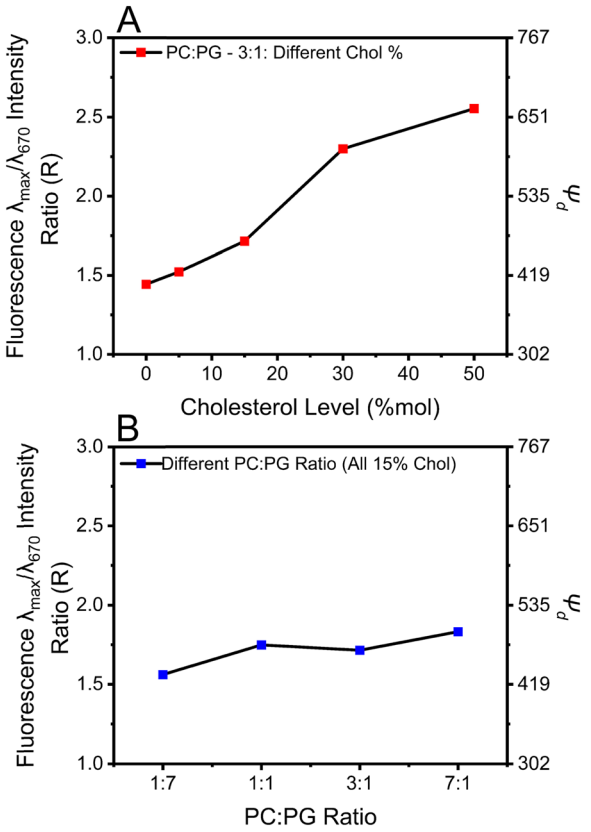

Fig. 4 Fluorescence intensity ratio, R, for estimating the transmembrane dipole potential (Ψ_d). (A) Liposomes with 3 : 1 POPC : POPG ratios but different cholesterol levels and (B) liposomes with the same cholesterol level (15%) but different POPC:POPG.

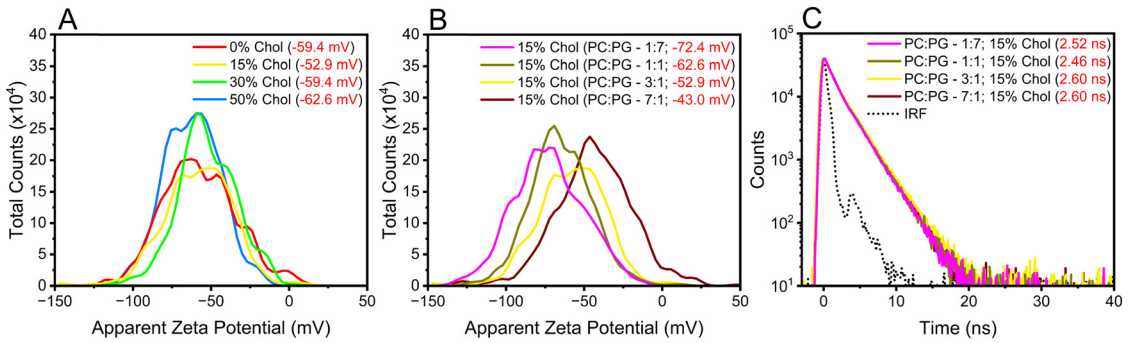

Fig. 3 (A) ζ-potential for the investigated liposomes with 3 : 1 POPC : POPG ratios but different cholesterol levels. (B) ζ-potential for the investigated liposomes with the same cholesterol level (15%) but different POPC : POPG and (C) their respective fluorescence lifetimes.

influence the fluorescence lifetime of DI-8-ANEPPS to a greater extent than changes in Ψ_d. This becomes more apparent when the fluorescence spectra of the mentioned samples are further contextualized. The changes in the Stoke shifts (~119 nm) and quantum yield of the liposomes when the POPC:POPG are modulated are minimal. In comparison, a sizable difference in the Stokes shift and quantum yield was obtained when cholesterol was increased from 0% (126 nm) to 15% (119 nm), see Table S1 (ESI†). In addition, these results align with previous studies where DI-8-ANEPPS is used to probe the impact of cholesterol levels on the orientational polarizability in relatively fluid membranes.[4,17] In that study, it was concluded that the cholesterol's effect in restricting the degree of movement (*i.e.*, increasing LO character) dominates over its effect on the local dipole strength.

In conclusion, it is possible to use the fluorescence lifetime DI-8-ANEPPS, a TICT dye, to inform about membrane fluidity. In the case of liposomes composed of POPC:POPG, increasing the cholesterol levels resulted in decreasing membrane fluidity, which manifested by a lengthening in the fluorescence lifetime of DI-8-ANEPPS concomitant with a quantum yield enhancement and a reduction in Stokes shifts due to LE dominating over TICT states. Note that increasing cholesterol levels in the membrane also resulted in increasing Ψ_d. However, changing the POPC:POPG ratios revealed that Ψ_d has minimal impact on the fluorescence lifetime of the DI-8-ANEPPS in comparison with the impact that membrane-rigidification has upon increasing cholesterol levels. Altogether, such photophysical response indicates that increasing the cholesterol levels in model membranes composed of POPC:POPG results in membranes with more LO phase character than Lα character, which can be sensed by coupling DI-8-ANEPPS with time-resolved fluorescence techniques.

Conflicts of interest

The authors declare no conflict of interest.

Acknowledgements

The Start-Up package provided by Indiana University Bloomington (IUB) to the corresponding author supported this research. We thank the Light Microscopy Imaging Center (LMIC) at Indiana University Bloomington for supporting image acquisition and analysis. We thank the Physical Biochemistry Instrumentation Facility (PBIF) and the Nanoscale Characterization Facility (NCF) for zeta-potential acquisition and analysis. We thank Professor Stephen Jacobson and Professor Yan Yu and their groups for their overall feedback on the project.

References

1 R. J. Clarke and D. J. Kane, Optical Detection of Membrane Dipole Potential: Avoidance of Fluidity and Dye-Induced Effects, *Biochim. Biophys. Acta, Biomembr.*, 1997, **1323**, 223–239.

2 S. Bandari, H. Chakraborty, D. F. Covey and A. Chattopadhyay, Membrane Dipole Potential Is Sensitive to Cholesterol Stereospecificity: Implications for Receptor Function, *Chem. Phys. Lipids*, 2014, **184**, 25–29, DOI: **10.1016/j.chemphyslip.2014.09.001**.

3 S. Haldar, R. K. Kanaparthi, A. Samanta and A. Chattopadhyay, Differential Effect of Cholesterol and Its Biosynthetic Precursors on Membrane Dipole Potential, *Biophys. J.*, 2012, **102**(7), 1561–1569, DOI: **10.1016/j.bpj.2012.03.004**.

4 R. A. Demel and B. De Kruyff, The Function of Sterols in Membranes, *Biochim. Biophys. Acta, Biomembr.*, 1976, **457**(2), 109–132, DOI: **10.1016/0304-4157(76)90008-3**.

5 Y. Zhang, Q. Li, M. Dong and X. Han, Effect of Cholesterol on the Fluidity of Supported Lipid Bilayers, *Colloids Surf., B*, 2020, 196, DOI: **10.1016/j.colsurfb.2020.111353**.

6 E. J. Fernández-Pérez, F. J. Sepúlveda, C. Peters, D. Bascuñán, N. O. Riffo-Lepe, J. González-Sanmiguel, S. A. Sánchez, R. W. Peoples, B. Vicente and L. G. Aguayo, Effect of Cholesterol on Membrane Fluidity and Association of Aβ Oligomers and Subsequent Neuronal Damage: A Double-Edged Sword, *Front. Aging Neurosci.*, 2018, **10**, 226, DOI: **10.3389/fnagi.2018.00226**.

7 P. Sarkar and A. Chattopadhyay, Membrane Dipole Potential: An Emerging Approach to Explore Membrane Organization and Function, *J. Phys. Chem. B*, 2022, **126**(24), 4415–4430, DOI: **10.1021/acs.jpcb.2c02476**.

8 H. Halimi and S. Farjadian, Cholesterol: An Important Actor on the Cancer Immune Scene, *Front. Immunol.*, 2022, **13**, 1057546, DOI: **10.3389/fimmu.2022.1057546**.

9 E. Ikonen, Cellular Cholesterol Trafficking and Compartmentalization, *Nat. Rev. Mol. Cell Biol.*, 2008, **9**(2), 125–138, DOI: **10.1038/nrm2336**.

10 S. T. Yang, A. J. B. Kreutzberger, J. Lee, V. Kiessling and L. K. Tamm, The Role of Cholesterol in Membrane Fusion, *Chem. Phys. Lipids*, 2016, **199**, 136–143, DOI: **10.1016/j.chemphyslip.2016.05.003**.

11 A. D. Juhl and D. Wüstner, Pathways and Mechanisms of Cellular Cholesterol Efflux—Insight From Imaging, *Front. Cell Dev. Biol.*, 2022, **10**, 834408, DOI: **10.3389/fcell.2022.834408**.

12 M. F. Vitha and R. J. Clarke, Comparison of Excitation and Emission Ratiometric Fluorescence Methods for Quantifying the Membrane Dipole Potential, *Biochim. Biophys. Acta, Biomembr.*, 2007, **1768**(1), 107–114, DOI: **10.1016/j.bbamem.2006.06.022**.

13 R. Youngworth and B. Roux, Simulating the Fluorescence of Di-8-ANEPPS in Solvents of Different Polarity, *J. Phys. Chem. B*, 2024, **128**(1), 184–192, DOI: **10.1021/acs.jpcb.3c02974**.

14 R. Youngworth and B. Roux, Simulating the Voltage-Dependent Fluorescence of Di-8-ANEPPS in a Lipid Membrane, *J. Phys. Chem. Lett.*, 2023, **14**(36), 8268–8276, DOI: **10.1021/acs.jpclett.3c01257**.

15 T. Starke-Peterkovic, N. Turner, P. L. Else and R. J. Clarke, Electric Field Strength of Membrane Lipids from Vertebrate Species: Membrane Lipid Composition and Na^+ -K^+-ATPase

Molecular Activity, *Am. J. Physiol. Regul., Integr. Comp. Physiol.*, 2005, **288**(3), R663–R670, DOI: 10.1152/ajpregu.00434.2004.

16 T. Starke-Peterkovic, N. Turner, M. F. Vitha, M. P. Waller, D. E. Hibbs and R. J. Clarke, Cholesterol Effect on the Dipole Potential of Lipid Membranes, *Biophys. J.*, 2006, **90**(11), 4060–4070, DOI: 10.1529/biophysj.105.074666.

17 G. Le Goff, M. F. Vitha and R. J. Clarke, Orientational Polarisability of Lipid Membrane Surfaces, *Biochim. Biophys. Acta, Biomembr.*, 2007, **1768**(3), 562–570, DOI: 10.1016/j.bbamem.2006.10.019.

18 B. Jiang, U. Umezaki, A. Augustine, V. M. Jayasinghe-Arachchige, L. F. Serafim, Z. M. S. He, K. M. Wyss, R. Prabhakar and A. A. Martí, Deconvoluting Binding Sites in Amyloid Nanofibrils Using Time-Resolved Spectroscopy, *Chem. Sci.*, 2023, **14**(5), 1072–1081, DOI: 10.1039/d2sc05418c.

19 D. Mondal, R. Dutta, P. Banerjee, D. Mukherjee, T. K. Maiti and N. Sarkar, Modulation of Membrane Fluidity Performed on Model Phospholipid Membrane and Live Cell Membrane: Revealing through Spatiotemporal Approaches of FLIM, FAIM, and TRFS, *Anal. Chem.*, 2019, **91**(7), 4337–4345, DOI: 10.1021/acs.analchem.8b04044.

20 R. J. R. J. Vázquez, H. Kim, P. M. P. M. Zimmerman and T. Goodson, Using Ultra-Fast Spectroscopy to Probe the Excited State Dynamics of a Reported Highly Efficient Thermally Activated Delayed Fluorescence Chromophore, *J. Mater. Chem. C*, 2019, **7**(14), 4210–4221, DOI: 10.1039/C8TC05957H.

21 R. J. Vázquez, J. H. Yun, A. K. Muthike, M. Howell, H. Kim, I. K. Madu, T. Kim, P. Zimmerman, J. Y. Lee and T. G. Iii, New Direct Approach for Determining the Reverse Intersystem Crossing Rate in Organic Thermally Activated Delayed Fluorescent (TADF) Emitters, *J. Am. Chem. Soc.*, 2020, **142**(18), 8074–8079, DOI: 10.1021/jacs.0c01225.

22 L. Fisher, R. J. Vázquez, M. Howell, A. K. Muthike, M. E. Orr, H. Jiang, B. Dodgen, D. R. Lee, J. Y. Lee, P. Zimmerman and T. Goodson, Investigation of Thermally Activated Delayed Fluorescence in Donor–Acceptor Organic Emitters with Time-Resolved Absorption Spectroscopy, *Chem. Mater.*, 2022, **34**(5), 2161–2175, DOI: 10.1021/acs.chemmater.1c03668.

23 R. R. Duncan, A. Bergmann, M. A. Cousin, D. K. Apps and M. J. Shipston, Multi-dimensional Time-correlated Single Photon Counting (TCSPC) Fluorescence Lifetime Imaging Microscopy (FLIM) to Detect FRET in Cells, *J. Microsc.*, 2004, **215**(1), 1–12, DOI: 10.1111/j.0022-2720.2004.01343.x.

24 C. Albrecht and R. Joseph, Principles of Fluorescence Spectroscopy, 3rd Edition, *Anal. Bioanal. Chem.*, 2008, **390**(5), 1223–1224, DOI: 10.1007/s00216-007-1822-x.

25 A. S. Kashirina, I. López-Duarte, M. Kubánková, A. A. Gulin, V. V. Dudenkova, S. A. Rodimova, H. G. Torgomyan, E. V. Zagaynova, A. V. Meleshina and M. K. Kuimova, Monitoring Membrane Viscosity in Differentiating Stem Cells Using BODIPY-Based Molecular Rotors and FLIM, *Sci. Rep.*, 2020, **10**(1), 14063, DOI: 10.1038/s41598-020-70972-5.

26 J. Liu, Z. Liu, F. Mi, Z. Yao, X. Fang, Y. Wang, Z. Zhao and C. Wu, Fluorescence Lifetime Multiplex Imaging in Expansion Microscopy with Tunable Donor–Acceptor Polymer Dots, *Chem. Biomed. Imaging*, 2023, **1**(6), 550–557, DOI: 10.1021/cbmi.3c00058.

27 J. Sankaran and T. Wohland, Fluorescence Strategies for Mapping Cell Membrane Dynamics and Structures, *APL Bioeng.*, 2020, **4**(2), 020901, DOI: 10.1063/1.5143945.

28 R. Datta, T. M. Heaster, J. T. Sharick, A. A. Gillette and M. C. Skala, Fluorescence Lifetime Imaging Microscopy: Fundamentals and Advances in Instrumentation, Analysis, and Applications, *J. Biomed. Opt.*, 2020, **25**(07), 1, DOI: 10.1117/1.JBO.25.7.071203.

29 K. Suhling, P. M. W. French and D. Phillips, Time-Resolved Fluorescence Microscopy, *Photochem. Photobiol. Sci.*, 2005, **4**(1), 13–22, DOI: 10.1039/b412924p.

30 L. E. Shimolina, A. A. Gulin, M. Paez-Perez, I. López-Duarte, I. N. Druzhkova, M. M. Lukina, M. V. Gubina, N. J. Brooks, E. V. Zagaynova, M. K. Kuimova and M. V. Shirmanova, Mapping Cisplatin-Induced Viscosity Alterations in Cancer Cells Using Molecular Rotor and Fluorescence Lifetime Imaging Microscopy, *J. Biomed. Opt.*, 2020, **25**(12), 1–16, DOI: 10.1117/1.jbo.25.12.126004.

31 L. Shimolina, A. Gulin, N. Ignatova, I. Druzhkova, M. Gubina, M. Lukina, L. Snopova, E. Zagaynova, M. K. Kuimova and M. Shirmanova, The Role of Plasma Membrane Viscosity in the Response and Resistance of Cancer Cells to Oxaliplatin, *Cancers*, 2021, **13**(24), 6165, DOI: 10.3390/cancers13246165.

32 N. V. Visser, A. Van Hoek, A. J. W. G. Visser, J. Frank, H.-J. Apell and R. J. Clarke, Time-Resolved Fluorescence Investigations of the Interaction of the Voltage-Sensitive Probe RH421 with Lipid Membranes and Proteins', *Biochemistry*, 1995, **34**, 11777–11784.

33 R. J. Vázquez, H. Kim, B. M. Kobilka, B. J. Hale, M. Jeffries-EL, P. Zimmerman and T. Goodson, Evaluating the Effect of Heteroatoms on the Photophysical Properties of Donor–Acceptor Conjugated Polymers Based on 2,6-Di(Thiophen-2-yl)Benzo[1,2-*b*:4,5-*B*′]Difuran: Two-Photon Cross-Section and Ultrafast Time-Resolved Spectroscopy, *J. Phys. Chem. C*, 2017, **121**(27), 14382–14392, DOI: 10.1021/acs.jpcc.7b01767.

34 Z. Cai, R. J. Vázquez, D. Zhao, L. Li, W. Lo, N. Zhang, Q. Wu, B. Keller, A. Eshun, N. Abeyasinghe, H. Banaszak-Holl, T. Goodson and L. Yu, Two Photon Absorption Study of Low-Bandgap, Fully Conjugated Perylene Diimide-Thienoacene-Perylene Diimide Ladder-Type Molecules, *Chem. Mater.*, 2017, **29**(16), 6726–6732, DOI: 10.1021/acs.chemmater.7b01512.

35 K. Pinkwart, F. Schneider, M. Lukoseviciute, T. Sauka-Spengler, E. Lyman, C. Eggeling and E. Sezgin, Nanoscale Dynamics of Cholesterol in the Cell Membrane, *J. Biol. Chem.*, 2019, **294**(34), 12599–12609, DOI: 10.1074/jbc.RA119.009683.

36 S. Muthusubramanian and S. K. Saha, Exploration of Twisted Intramolecular Charge Transfer Fluorescence Properties of *Trans*-2-[4-(Dimethylamino)Styryl]Benzothiazole to

Characterize the Protein-Surfactant Aggregates, *J. Lumin.*, 2012, **132**(8), 2166–2177, DOI: **10.1016/j.jlumin.2012.03.053**.

37 A. Marczak, Fluorescence Anisotropy of Membrane Fluidity Probes in Human Erythrocytes Incubated with Anthracyclines and Glutaraldehyde, *Bioelectrochemistry*, 2009, **74**(2), 236–239, DOI: **10.1016/j.bioelechem.2008.11.004**.

38 W. Zhao, T. Róg, A. A. Gurtovenko, I. Vattulainen and M. Karttunen, Atomic-Scale Structure and Electrostatics of Anionic Palmitoyloleoylphosphatidylglycerol Lipid Bilayers with Na^+ Counterions, *Biophys. J.*, 2007, **92**(4), 1114–1124, DOI: **10.1529/biophysj.106.086272**.

39 G. W. Feigenson, Phase Behavior of Lipid Mixtures, *Nat. Chem. Biol.*, 2006, **2**(11), 560–563, DOI: **10.1038/nchembio1106-560**.

40 L. Jin, A. C. Millard, J. P. Wuskell, X. Dong, D. Wu, H. A. Clark and L. M. Loew, Characterization and Application of a New Optical Probe for Membrane Lipid Domains, *Biophys. J.*, 2006, **90**(7), 2563–2575, DOI: **10.1529/biophysj.105.072884**.

41 G. W. Feigenson, Phase Boundaries and Biological Membranes, *Annu. Rev. Biophys. Biomol. Struct.*, 2007, 63–77, DOI: **10.1146/annurev.biophys.36.040306.132721**.

42 G. W. Feigenson, Phase Diagrams and Lipid Domains in Multicomponent Lipid Bilayer Mixtures, *Biochim. Biophys. Acta, Biomembr.*, 2009, 47–52, DOI: **10.1016/j.bbamem.2008.08.014**.

43 M. M. Domingues, P. S. Santiago, M. A. R. B. Castanho and N. C. Santos, What Can Light Scattering Spectroscopy Do for Membrane-Active Peptide Studies?, *J. Pept. Sci.*, 2008, 394–400, DOI: **10.1002/psc.1007**.

44 J. M. Freire, M. M. Domingues, J. Matos, M. N. Melo, A. S. Veiga, N. C. Santos and M. A. R. B. Castanho, Using Zeta-Potential Measurements to Quantify Peptide Partition to Lipid Membranes, *Eur. Biophys. J.*, 2011, **40**(4), 481–487, DOI: **10.1007/s00249-010-0661-4**.

45 K. Redmann, H.-L. Jenssen and H.-J. Köhler, Experimental and Functional Changes in Transmembrane Potential and Zeta Potential of Single Cultured Cells, *Exp. Cell Res.*, 1974, **87**(2), 281–289, DOI: **10.1016/0014-4827(74)90482-0**.